

Adhithiaram Hariharan – Technical Portfolio

About Me

My work is at the intersection of structural mechanics, fluid dynamics, thermal modeling, and data-driven methods. I approach engineering problems by first understanding the physical behavior of the system and then translating it into a computational framework that captures key interactions without losing realism. With a strong foundation in solid mechanics and CFD, I have contributed to the simulation and design of real-world systems, from vehicle chassis under crash loads to temperature-driven deformation in weld zones.

Much of my experience lies in the practical use of tools like Abaqus, Ansys, OpenFOAM, and MATLAB to run analyses and validate and finalize design decisions. I have worked on static and dynamic FEA, modal analysis, turbulent flow modeling, and coupled thermo-mechanical problems. I am comfortable working from geometry cleanup and meshing all the way to results interpretation and model validation.

This portfolio compiles projects where simulation wasn't just used to visualize results, but to guide design, support engineering judgment, and explain the physics that drive performance.

Contents

Design and Fabrication of an All-Terrain Vehicle	2
Control-Oriented Modeling of X-HALE Aircraft	4
River Flow Simulations Using OpenFOAM	6
Reduced-Order Modeling of Friction Stir Welding Process	8
Appendix: Equations, Detailed Process and Other results	10

Design and Fabrication of an All-Terrain Vehicle

Team: PSI Racing, National Institute of Technology Tiruchirappalli

Introduction

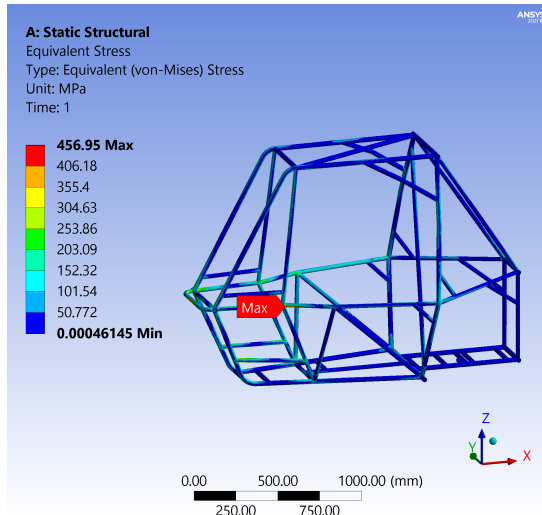
The All-Terrain Vehicle (ATV) developed for BAJA SAE competition was designed for optimal durability, dynamic performance, and manufacturability. The design effort was geared towards robustness and safety. I used ANSYS to validate performance under extreme loading. The project covered the complete product lifecycle from CAD to CAE, CNC fabrication, and DFMEA/DVP.



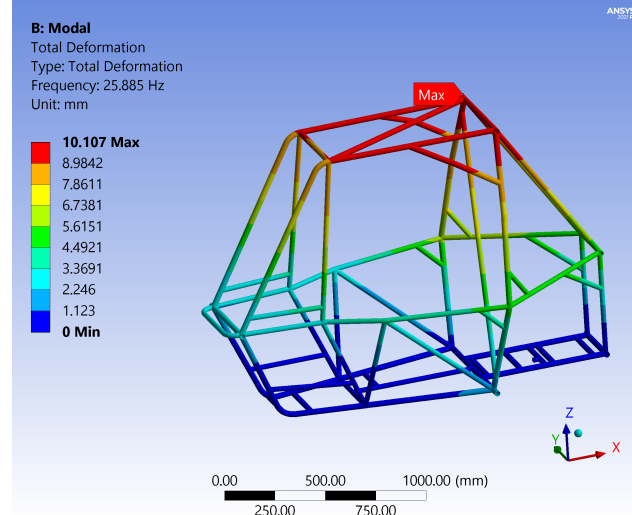
Structural and Modal Analysis

Chassis design focused on maximizing structural rigidity while minimizing weight. Simulations included static structural tests under frontal, rear, side, torsional, and bump loads, as well as modal analysis with six modes (Effective Mass Participation Factor is 1 at the sixth mode, which means the whole chassis experience vibrations).

The chassis was constructed using AISI 4130 tubing, resulting in a final weight of 33 kg. Under various crash scenarios, the factor of safety ranged from 1.1 to 4.0, ensuring structural integrity in impact conditions. Modal analysis revealed natural frequencies ranging from 22 to 83 Hz across primary modes, all below the operating engine frequency range (150 to 290 Hz).



(a) Static deformation under frontal impact



(b) First mode shape from modal analysis

Thermal and CFD Analysis

Thermal simulations were run on the rotor, CVT cover were done in both Ansys Fluent and OpenFOAM. CFD analysis was done for gearbox (for lubrication), and chassis (for drag analysis).

A 50 CFM (50 cubic feet of air per minute) fan was modeled using OpenFOAM. A steady-state thermal solution was used to visualize heat flow and vortex shedding.

CFD Setup:

- Inlet: Flowrate = 50 CFM, Temperature = 363K
- Outlet: Pressure fixedValue
- RPM of rotating elements: 3000 rpm

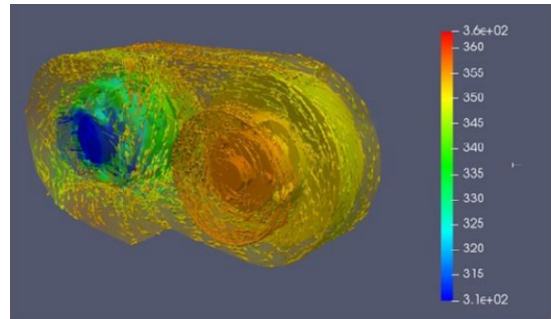


Figure 2: Flow path contours of CVT

Outputs:

- Temperature distribution across CVT cover
- Velocity streamlines inside CVT enclosure

Topology Optimization

Topology optimization was performed on the rear differential casing and rotor designs to reduce mass while maintaining safety margins. Optimized gear had a 46% weight reduction.

More design and analysis results are shown in **Appendix 1**



Figure 3: Optimized gear structure

CAM Manufacturing

Several components including the suspension upright (knuckle), engine mounts, and brake pedal were manufactured in-house using CNC milling. Pipe model chassis prototypes were used to validate ergonomics and perform physical clearances prior to full assembly.

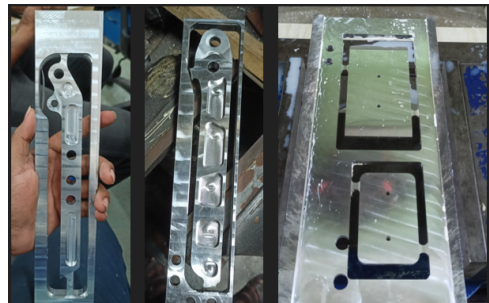


Figure 4: CNC Milling of brake pedal

Overall Project Timeline

The development process began with an analysis of previous designs, followed by defining new design objectives. Each subsystem was designed and analyzed individually, after which a full CAD assembly was created to validate packageability and serviceability. A chassis prototype was fabricated to perform ergonomic checks. Manufacturing commenced with chassis fabrication involving drilling, cutting, profiling, and fixture-assisted welding, followed by the integration of other subsystems post-CAM machining. The completed ATV underwent static and dynamic data acquisition tests under various loading conditions.

Other Roles & Contributions: I generated detailed engineering drawings, collaborated with cross-functional teams and held design reviews for assembly layout. I have successfully managed to build the ATV within project timeline, budget and also mentored new team members.

Control-Oriented Low-Order Modeling of the X-HALE Aircraft

Mentor: Prof. Carlos E. S. Cesnik

Lab: Active Aeroelasticity and Structures Research Lab (A2SRL), University of Michigan

Introduction

Very flexible aircraft (VFA) experience large structural deformations, coupling its elastic nature and flight dynamics significantly. Traditional rigid-body models fail to capture these deformation effects, especially for high-altitude long-endurance (HALE) aircraft, where geometrical nonlinearities dominate the response. This project addresses these limitations through a bottom-to-top (B2T) reduced-order modeling framework that captures nonlinear aeroelastic behavior in a control-oriented environment at real time.

Modeling Approach

The B2T approach enriches traditional 6-DOF rigid-body equations with additional flexible degrees of freedom based on strain modes. Nonlinear structural and aerodynamic terms are extracted from high-fidelity nonlinear aeroelastic solver (UM/NAST) and neural networks are trained on this data. **Appendix 2** has the equations and Neural net mapping explained.

The overall process involves trimming the aircraft, performing modal decomposition to extract dominant modes, and performing residualization to retain the influence of truncated modes. Neural networks are used to approximate the nonlinear structural and aerodynamic terms based on the reduced state space. This enables real-time simulation capability.

Simulation Setup

The test platform used is the University of Michigan's X-HALE, a 6-meter span aircraft capable of large tip deflections (more than 40% of the span). This makes X-HALE a representative model for HALE-class aircraft exhibiting coupled nonlinear aeroelastic effects.



Figure 5: X-HALE in experimental and flight conditions, showing structural deformation

- Trim Condition: 30 m altitude, 14 m/s cruise conditions
- Control Input: 0.5-degree pitch elevator doublet (excited from 1 to 7 seconds)
- Modes Retained: 4 out of 64 strain modes
- Training Data: Strain modes, velocities, angles, and control inputs

Results

The reduced-order model is tested for roll and pitch maneuvers. Using only 4 strain modes, the model captures the essential dynamics with good agreement to UM/NAST. The comparison of roll (p), pitch (q), and yaw (r) rates and their corresponding Euler angles (ϕ, θ, ψ) during maneuver shows similar trends. The B2T model achieves a 40 times speed up compared to the 'full order' dynamic reference solution generated through UM/NAST.

In the figure below, solid lines represent the full-order high-fidelity simulation results, while dotted lines correspond to the reduced-order B2T predictions.

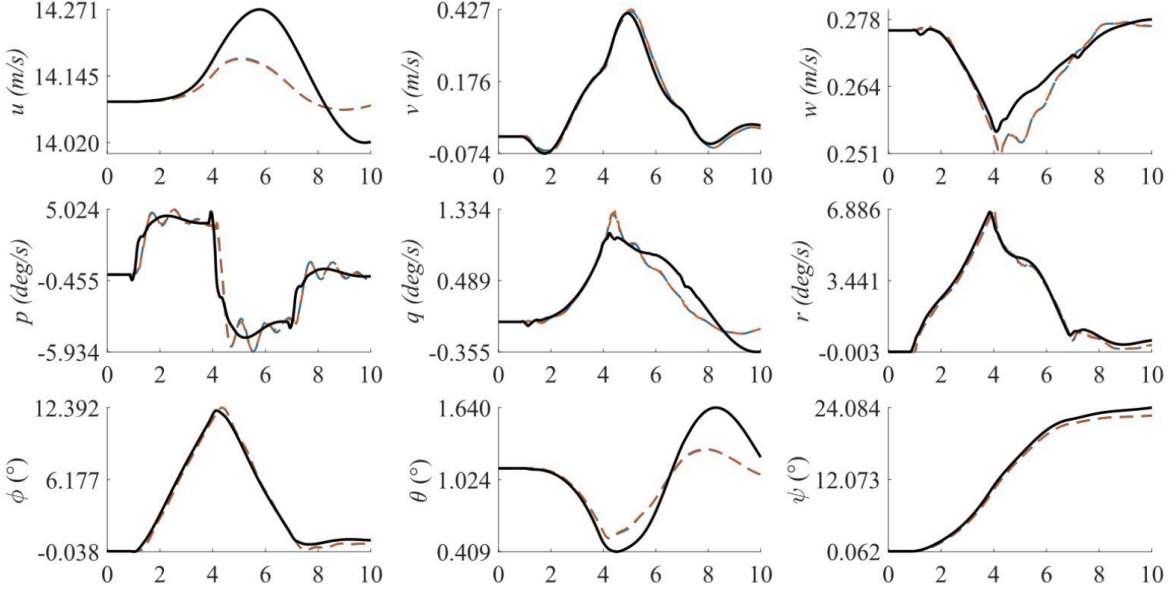


Figure 6: Comparison results between B2T (dotted) and full-order model (solid)

Conclusion

This research demonstrates a real-time capable, control-oriented modeling approach for VFA using the B2T framework. The X-HALE aircraft is used as the testbed, with reduced-order models showing high accuracy and substantial speed-up. The neural networks trained on flexible structural and aerodynamic terms capture the nonlinear transitions and control response.

River Flow Simulations Using OpenFOAM

Mentor: Prof. Narasimalu Srikanth

Lab: Energy Research Institute, Nanyang Technological University

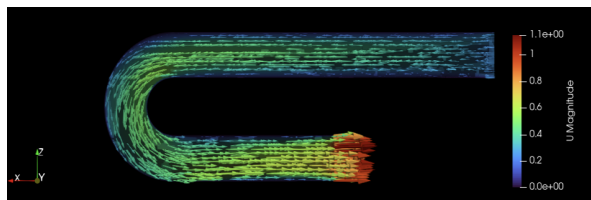
Introduction

This project involved the study of free-surface flows in complex river geometries such as meanders, confluences, and curved bends using OpenFOAM. The objective was to simulate the flow behavior of natural water bodies to analyze secondary flows, wall-bounded turbulence, and velocity field distortions. The simulations were aimed at characterizing ambient turbulence prior to tidal turbine deployment and supporting data-driven design of hydrodynamic systems.

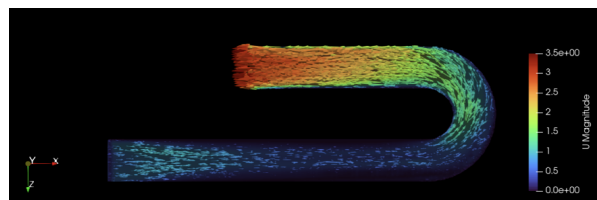
Simulation Approach

CFD simulations were carried out using OpenFOAM's `interFoam` solver for free-surface flows and `simpleFoam` for rigid-lid approximations. The $k-\omega$ SST RANS turbulence model was used throughout. River topography was reconstructed from bathymetric measurements and processed in MATLAB for use in meshing and boundary definition.

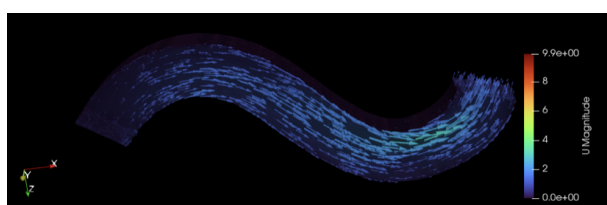
Simulation setup: 20-second transient simulation, inlet velocity = 0.25 m/s, water depth = 0.3 m, rigid-lid depth = 0.058 m. Turbulence modeled using $k-\omega$ SST. Results below compare both flow types under identical conditions.



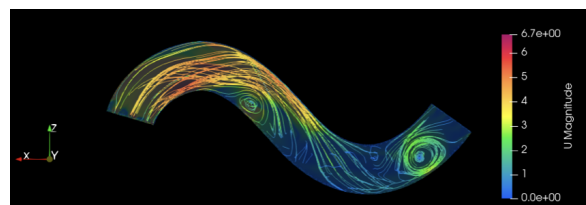
(a) Free-Surface Flow (Curved Surface Flow)



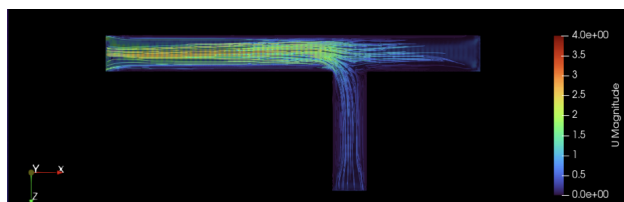
(b) Rigid-Lid Approximation (Curved Surface Flow)



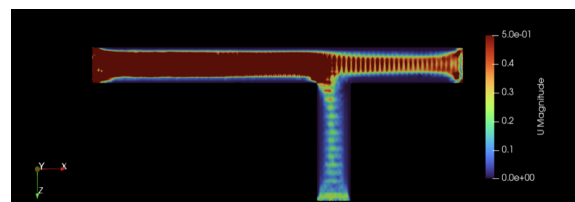
(a) Free-Surface Flow (Meandering Flow)



(b) Rigid-Lid Approximation (Meandering Flow)



(a) Free-Surface Flow (Confluent Flow)



(b) Rigid-Lid Approximation (Confluent Flow)

The Free-Surface flow is modeled using the Volume of Fluid method. The Rigid-Lid Model (RLM) produces higher velocity magnitudes due to the absence of surface deformation, concentrating the pressure gradient into in-plane flow. In contrast, the Free-Surface Model (FSM) dissipates part of the energy into vertical motion and surface elevation, resulting in lower horizontal velocities.

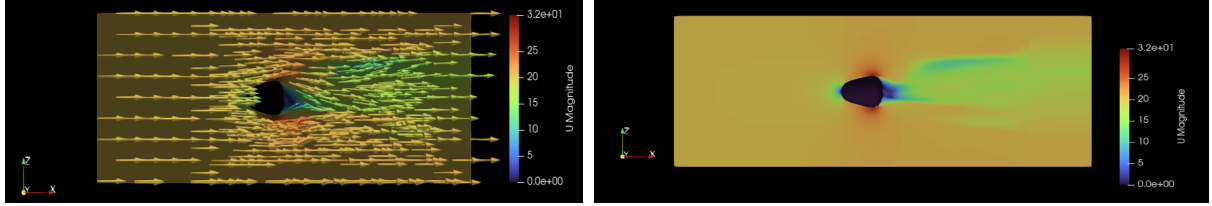
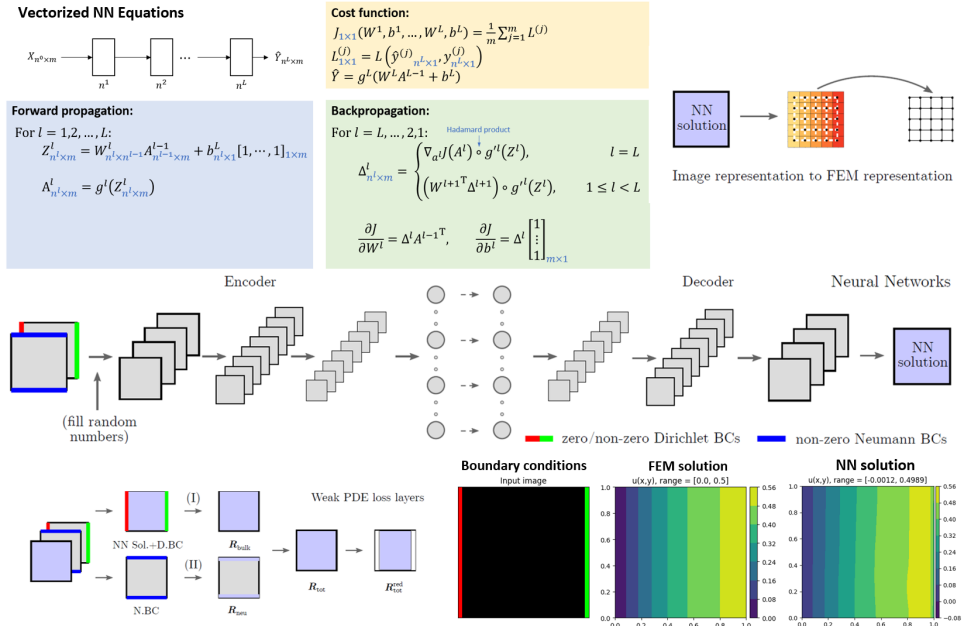


Figure 10: Flow over a rock

CNN-Based Surrogate Modeling

To reduce the computational cost associated with high-fidelity CFD simulations of river flow, a surrogate model was developed using Convolutional Neural Network (CNN). To validate the idea, the method was first tested on a 2D Poisson equation using a custom finite element solver, solving $\nabla^2 u + 1 = 0$ under varied boundary conditions. **Appendix 3** has the CNN process explained.



Future Work

This surrogate modeling framework will be extended to actual river flows. A *U-Net CNN architecture* is trained on OpenFOAM results of meandering river flows. Inputs were 2D maps encoding geometry and boundary conditions, while outputs were full velocity fields after 20 seconds of simulation.

Reduced-Order Modeling of the Friction Stir Welding Process

Mentor: Prof. Surjya Kanta Pal

Lab: Friction Stir Welding Laboratory - Indian Institute of Technology, Kharagpur

Introduction

Friction Stir Welding (FSW) is a solid-state joining technique in which a rotating tool with a pin and shoulder is plunged into the interface of two workpieces and traversed along the weld line. The process generates heat through friction and plastic deformation, softening the material and enabling it to flow around the tool to form a high-quality weld without melting. This solid-state nature reduces defects such as voids and porosity, while also minimizing residual stress. FSW is particularly suitable for aluminum and other non-ferrous alloys. However, the multi-physical and nonlinear nature of FSW makes it challenging to simulate efficiently.

The objective of this work is to develop a reduced-order model (ROM) for the FSW process to enable real-time predictions of material deformation and stress for varying process parameters. A ROM is constructed by mapping the simulation-based outputs from ABAQUS to corresponding input parameters. This model will serve as a predictive tool for evaluating weld quality and identifying failure-prone conditions.

FSW Analysis

The process was simulated using the Coupled Eulerian-Lagrangian (CEL) technique in ABAQUS to accurately model large deformations and material flow. The setup consists of a rigid tool and a deformable aluminum workpiece and is done in three stages: plunging (0–3 s), dwelling (3–3.5 s), and welding (3.5–9 s). Material properties were defined as temperature-dependent, and heat generation was modeled through applied pressures and rotational/translational tool velocities. Outputs included temperature and stress distributions along the weld zone. Due to the high computational cost of CEL simulations, model order reduction was adopted.

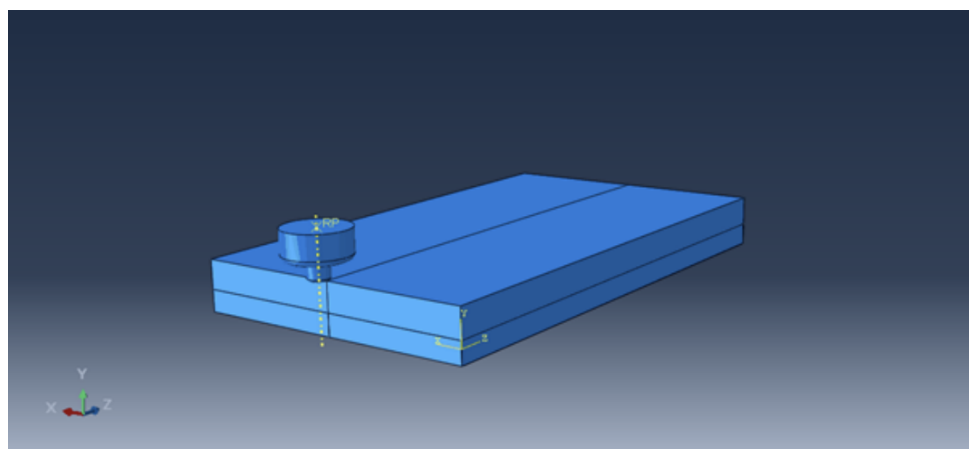


Figure 11: CAD modeling done using CATIA

Appendix 4 presents the governing equations for the POD-Galerkin-based ROM implemented in MATLAB. ABAQUS and MATLAB are interfaced using a Python wrapper to extract time-varying outputs.

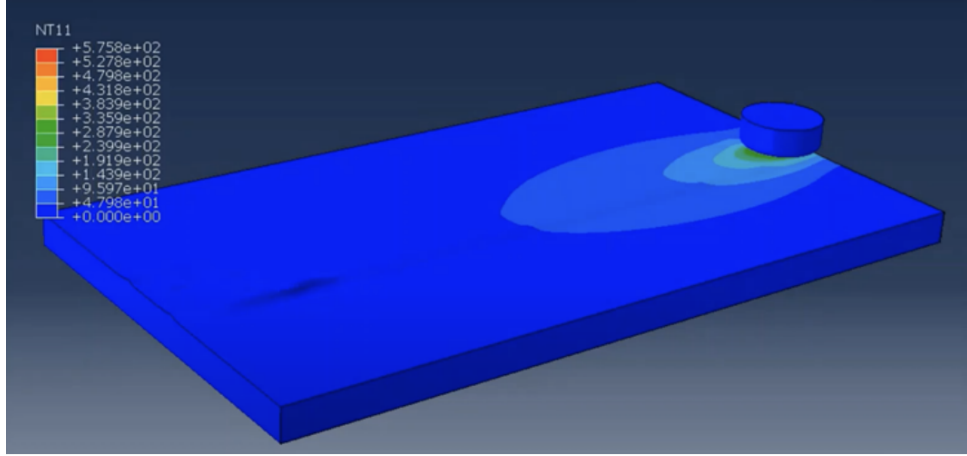


Figure 12: Temperature distribution from CEL simulation

Results

The figure below shows a spatiotemporal contour plot of temperature along a 100 mm straight weld path over 9 seconds, capturing the plunging, dwelling, and welding stages. The ROM results demonstrate close agreement with the full-order model, with reduced computational complexity. Reconstructions using 2, 4, and 10 POD modes were compared to the original full-field simulation to validate mode retention efficiency.

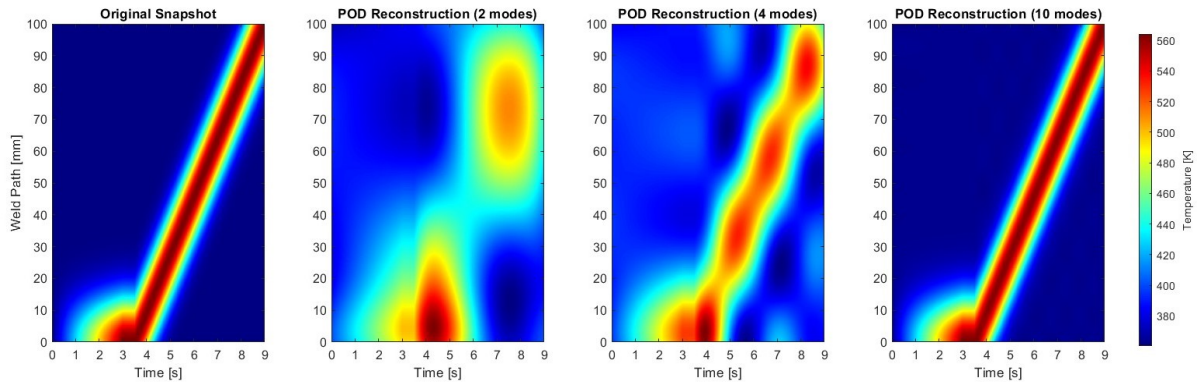
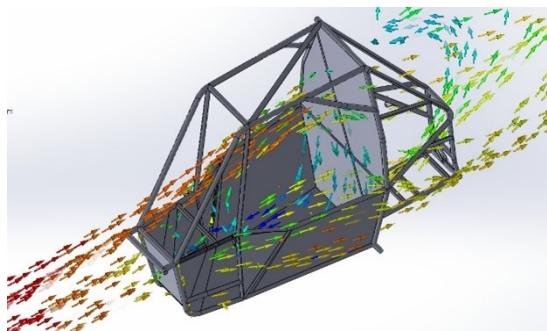


Figure 13: Temperature contour comparison: original vs. POD-reconstructed (2, 4, 10 modes)

Future Work

The reduced-order model is expected to provide a speed-up of approximately 70% relative to the high-fidelity ABAQUS CEL simulations, while retaining sufficient accuracy for use in control-oriented and design optimization workflows. Future developments will extend this model using snapshot matrices that include displacement (U), pressure (P), spatial coordinates (x), and temperature (T).

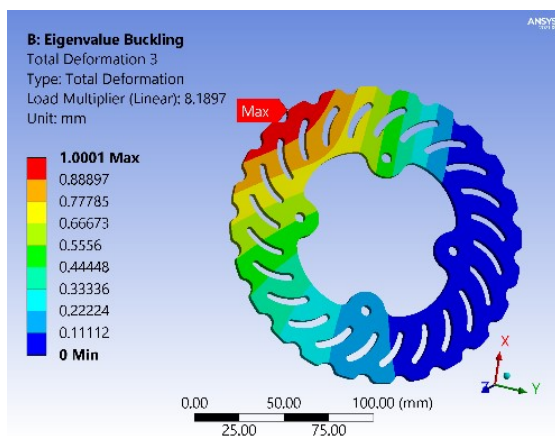
Appendix 1: Mechanical Design and Analysis



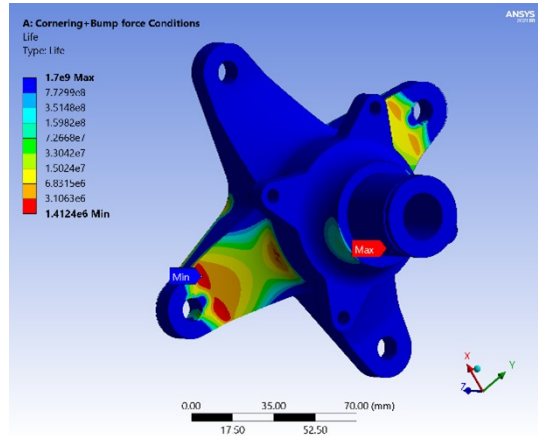
CFD analysis for placement of CVT duct - Analysed velocity fields near CVT and brake rotors.



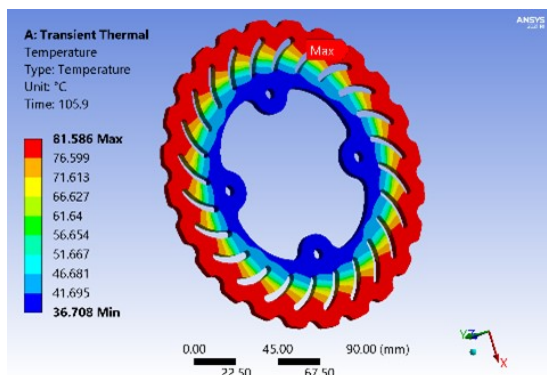
Brake Rotor CFD - Analysed the convective cooling rates due to air flow (vent placement)



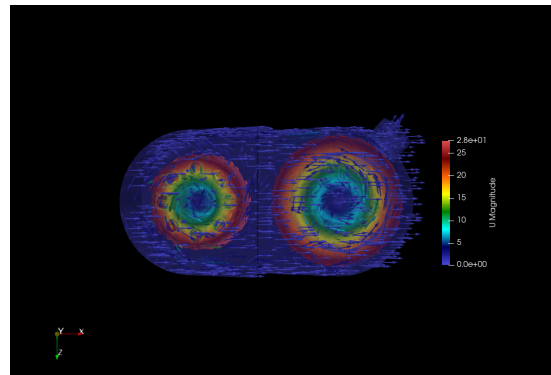
Buckling load multiplier * Applied Torque load = Critical buckling load used on static structural



Fatigue Analysis of Hub prone to repetitive bump and corner forces



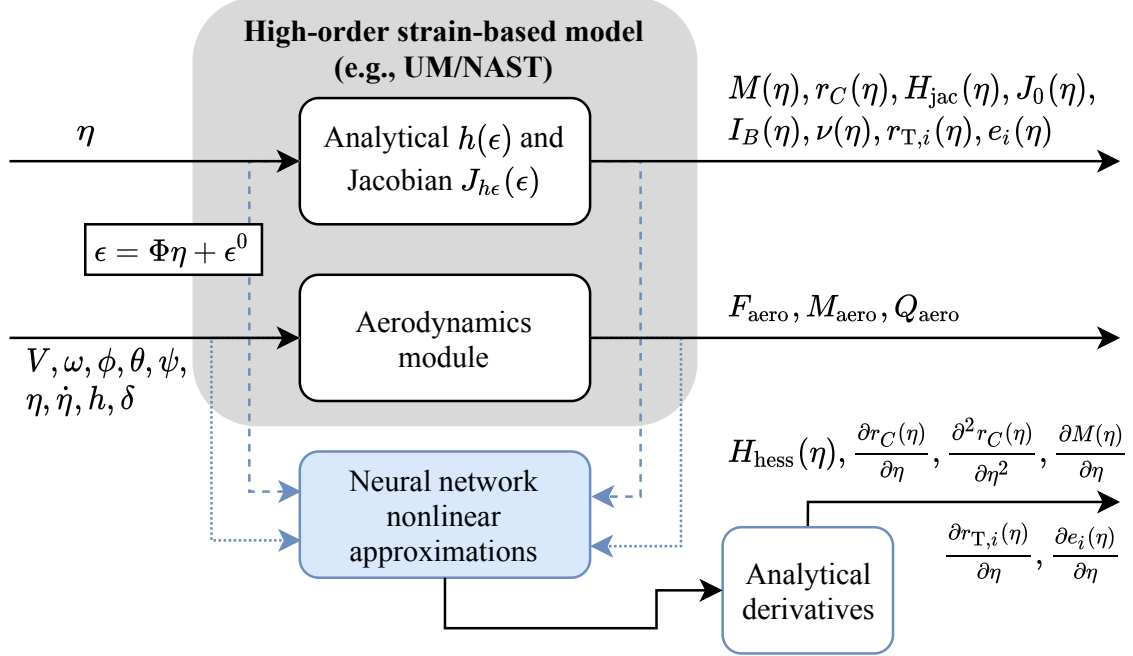
Transient Thermal Analysis of Rotor - Analysed Temperature distribution under braking loads



Initial Flow conditions for CVT CFD analysis - To decide placement of duct or electronic fan

Appendix 2: B2T Equations of Motion

For each input parameter of B2T model, a set of scaled training data are created (training data samples), and the corresponding output data are generated using UM/NAST. The neural networks are trained with these input/output pairs. The trained neural networks are used to generate the nonlinear structural and aerodynamic terms for solving the EOM for a new flight condition.



The equations of motion (EOM) is shown below:

$$E \frac{d}{dt} \begin{Bmatrix} V \\ \omega \\ \dot{\eta} \\ \eta \end{Bmatrix} = - \begin{Bmatrix} m\tilde{\omega}V + m\dot{\eta}^\top \frac{\partial^2 r_C(\eta)}{\partial \eta^2} \dot{\eta} + 2m\tilde{\omega} \frac{\partial r_C(\eta)}{\partial \eta} \dot{\eta} + m\tilde{\omega}^2 r_C(\eta) \\ m\tilde{r}_C(\eta)(\tilde{\omega}V) + \dot{\eta}^\top H_{\text{hess}}(\eta) \dot{\eta} + 2(J_0(\eta)\dot{\eta})\omega + \tilde{\omega}I_B(\eta)\omega \\ m \left(\frac{\partial r_C(\eta)}{\partial \eta} \right)^\top (\tilde{\omega}V) + \frac{1}{2}\dot{\eta}^\top \frac{\partial M}{\partial \eta} \dot{\eta} + 2(\nu(\eta)\dot{\eta})\omega - \omega^\top J_0(\eta)\omega + K\eta \\ -\dot{\eta} \end{Bmatrix} + \begin{Bmatrix} F_g + F_{\text{aero}} + F_{\text{thrust}} \\ M_g + M_{\text{aero}} + M_{\text{thrust}} \\ Q_g + Q_{\text{aero}} + Q_{\text{thrust}} \\ 0 \end{Bmatrix},$$

where

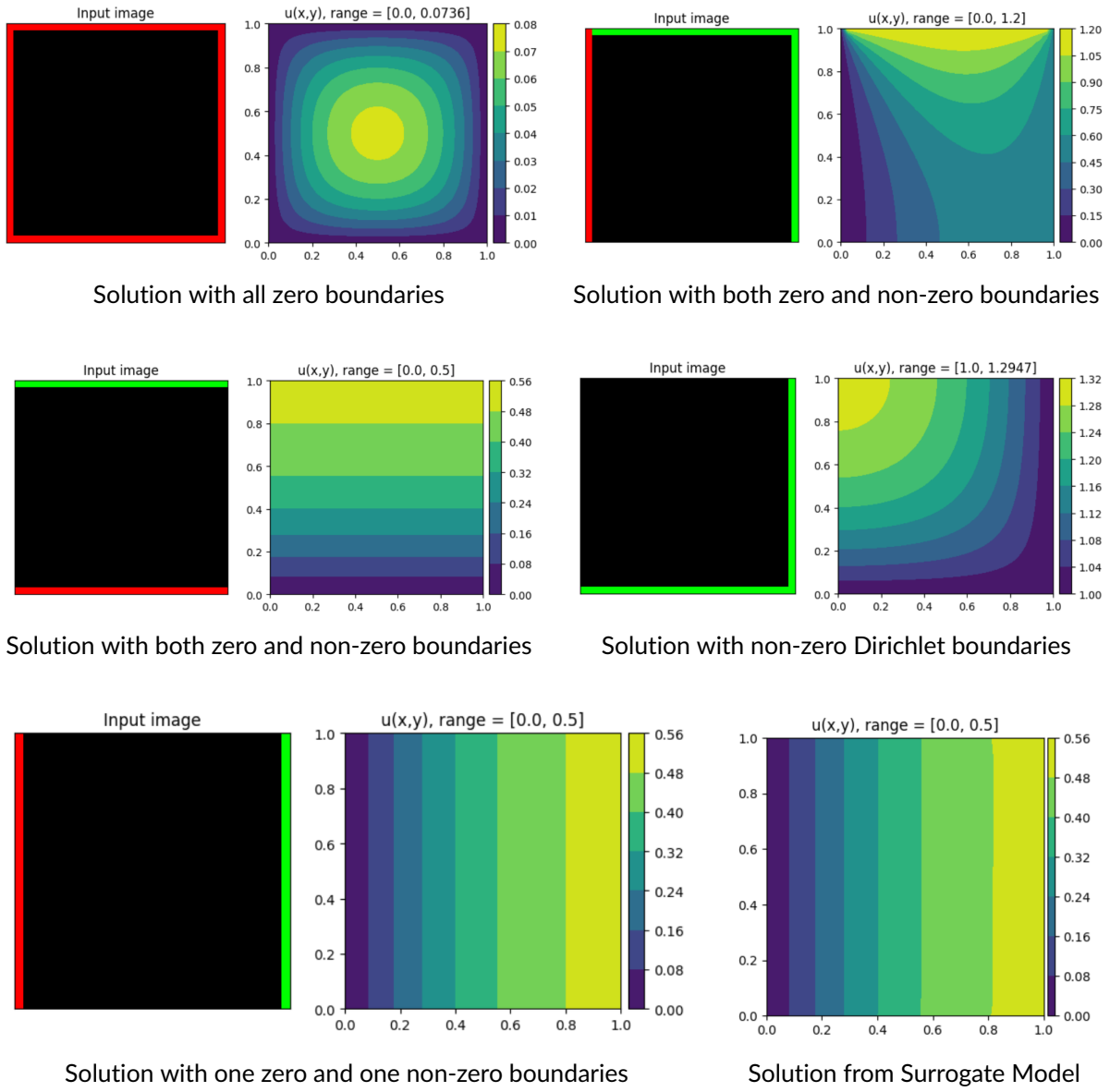
$$E = \begin{bmatrix} m & -m\tilde{r}_C(\eta) & m \frac{\partial r_C(\eta)}{\partial \eta} & 0 \\ m\tilde{r}_C(\eta) & I_B(\eta) & H_{\text{jac}}(\eta) & 0 \\ m \left(\frac{\partial r_C(\eta)}{\partial \eta} \right)^\top & H_{\text{jac}}^\top(\eta) & M(\eta) & 0 \\ 0 & 0 & 0 & I_n \end{bmatrix}.$$

Appendix 3: Surrogate Modeling of FEM/CFD simulations

The surrogate was implemented as a convolutional neural network (CNN) using the TensorFlow framework. The PDE $\nabla^2 u + 1 = 0$ was solved using a custom finite element method. A convolutional autoencoder was trained on a dataset of FEM-generated solutions under varying boundary conditions. The network minimized the residual of the PDE in its loss function and learned to map boundary conditions to solution fields. CNN training data was 5000 images and batch size of 32. The learning rate was 10^{-3} . The training took 17mins on CPU and the validation loss reached 0.009 and training loss was 0.0085.

Input Training Data and final ML-PDE solution

The red color shows the Dirichlet boundary condition with value of zero and the green color shows the Dirichlet boundary condition with non-zero value.



Appendix 4: POD-Galerkin ROM Equations

The full-order finite element model of the FSW process can be represented as a second-order differential system:

$$M\ddot{x}(t) + C\dot{x}(t) + Kx(t) = F(t)$$

where M , C , and K are the mass, damping, and stiffness matrices respectively, $x(t)$ is the state vector, and $F(t)$ is the input force vector. In the context of FSW, $F(t)$ includes both mechanical loading (pressure, tool forces) and thermal loading derived from temperature distributions, such as frictional heat.

To construct a reduced-order model, displacement data from a high-fidelity simulation is collected as *snapshots*. Each snapshot $x_i \in \mathbb{R}^{3N}$ is a displacement vector of all degrees of freedom (3 per node) at a specific time step t_i . These are assembled into a snapshot matrix:

$$X = [x_1, x_2, \dots, x_n] \in \mathbb{R}^{3N \times n}$$

where N is the number of nodes in the mesh, and n is the number of time steps.

Proper Orthogonal Decomposition (POD) is used to extract dominant spatial modes of the system by performing Singular Value Decomposition (SVD):

$$X = U\Sigma V^T$$

where U contains orthonormal spatial modes, Σ contains singular values, and V encodes temporal weights. A reduced basis Φ is then selected by truncating U to the first r dominant modes:

$$\Phi = U(:, 1:r)$$

Applying Galerkin projection to the original system, the reduced-order model becomes:

$$M_r\ddot{q}(t) + C_r\dot{q}(t) + K_rq(t) = \Phi^T F(t)$$

where the reduced matrices are:

$$M_r = \Phi^T M \Phi, \quad C_r = \Phi^T C \Phi, \quad K_r = \Phi^T K \Phi$$

and $q(t) \in \mathbb{R}^r$ are the generalized coordinates in the reduced subspace.

This reduced-order system captures the dominant dynamics of the full model and can be efficiently integrated in MATLAB for real-time simulation, control, or parametric studies. Temperature-dependent stiffness or damping can be incorporated by constructing multiple reduced models or enriching the basis using temperature-tagged snapshots.

Separate POD bases may be computed for temperature and displacement fields due to their differing spatial behaviors. Each field is then projected independently onto its corresponding reduced basis for reconstruction.